Development of precision Wolter mirrors for future solar x-ray observations

Taro Sakao*[a,g], Satoshi Matsuyama[b], Ayumi Kime[b], Takumi Goto[b], Akihiko Nishihara[b], Hiroki Nakamori[b], Kazuto Yamauchi[b], Yoshiki Kohmura[c], Akira Miyake[d], Hirokazu Hashizume[e], Tadakazu Maezawa[e], Yoshinori Suematsu[f], and Noriyuki Narukage[f]

[a]Institute of Space and Astronautical Science, Japan Aerospace Exploration Agency, 3-1-1 Yoshinodai, Chuo-ku, Sagamihara, Kanagawa 252-5210, Japan;
[b]Department of Precision Science and Technology, Graduate School of Engineering, Osaka University, 2-1 Yamada-oka, Suita, Osaka 565-0871, Japan
[c]SPring-8/RIKEN, 1-1-1 Kouto, Sayo-cho, Sayo, Hyogo 679-5148, Japan
[d]Canon Inc., 20-2 Kiyohara-Kogyodanchi, Utsunomiya 321-3292, Japan
[e]Natsume Optical Corp., 1200-29 Kawaji, Iida, Nagano 399-2431, Japan
[f]National Astronomical Observatory of Japan, 2-21-1 Osawa, Mitaka, Tokyo 181-8588, Japan
[g]Department of Space and Astronautical Science, School of Physical Sciences, The Graduate University for Advanced Studies (SOKENDAI), 3-1-1 Yoshinodai, Chuo-ku, Sagamihara, Kanagawa 252-5210, Japan

ABSTRACT

High resolution imagery of the solar X-ray corona provides a crucial key to understand dynamics and heating processes of plasma particles there. However, X-ray imagery of the Sun with sub-arcsecond resolution has yet to be conducted due to severe technical difficulty in fabricating precision Wolter mirrors. For future X-ray observations of the Sun's corona, we are attempting to realize precision Wolter mirrors with sub-arcsecond resolution by adopting advanced surface polish and metrology methods based on nano-technology to sector mirrors which consist of a portion of an entire annulus. Following fabrication of the first engineering mirror and subsequent evaluation on the X-ray focusing performance in 2013, the second engineering mirror was made with improvements in both precision polish and metrology introduced. Measurement of focusing performance on the second mirror at SPring-8 synchrotron facility with 8 keV X-rays has demonstrated that the FWHM size of the PSF core reached down to 0.2" while its HPD (Half Power Diameter) size remained at ~3" due to the presence of small-angle scatter just outside of the core. Also, there was notable difference in the focal length between sagittal and meridional focusing which could have been caused by an error in the sag in the meridional direction of <10 nm in the mirror area. Further improvements to overcome these issues have been planned for the next engineering mirror.

Keywords: Wolter mirror, X-ray telescope, solar corona, sub-arcsecond imagery, synchrotron X-rays, coherent X-rays

1. INTRODUCTION

The outer atmosphere of the Sun, the solar corona, is filled with plasmas whose temperature reaching, or even exceeding, 1 MK. The interplay between these plasma particles and magnetic fields originated from the surface of the Sun makes the corona highly dynamic including large-scale restructuring of the magnetic field[1], creation of super-hot (exceeding ~30 MK) plasmas and acceleration of particles during flares[2,3], gigantic mass ejections towards the interplanetary space[4], as well as heating of the corona itself[5]. Recent observations in EUV wavelengths from space have demonstrated that there are sub-arcsecond structures in the corona present and that such fine structures are responsible for supplying hot materials upward into the corona[6] and that they could constitute magnetic structure of the corona in the form of braided magnetic field lines[7].

*sakao@solar.isas.jaxa.jp; www.isas.jaxa.jp/e/, www.isas.jaxa.jp/sokendai/e

Optics for EUV, X-Ray, and Gamma-Ray Astronomy VII, edited by Stephen L. O'Dell, Giovanni Pareschi,
Proc. of SPIE Vol. 9603, 96030U · © 2015 SPIE · CCC code: 0277-786X/15/$18 · doi: 10.1117/12.2188905

As soft X-rays (with energy range from < ~1 keV to ~10 keV) can efficiently trace energized electrons in the corona, they are particularly suited for observing high energy processes (such as creation of high temperature plasmas well beyond 20 MK and acceleration of plasma particles) and their relationship with the associated magnetic structures in the corona. However, sub-arcsecond imagery in the soft X-ray range with Wolter I optics[8] has so far remained extremely difficult due to severe requirements on the surface figure profile for the mirror[9], demanding years of polishes hence resulting in huge amount of cost. As a result, sub-arcsecond imagery for astrophysical applications has so far only been accomplished by *Chandra* mission[10], but has never been made for the Sun.

With recent advances in precise surface metrology and precision polish, we have been attempting to realize Wolter I grazing-incidence X-ray mirrors for future solar observations with sub-arcsecond resolution (in terms of half-power diameter; HPD), by means of direct polishing onto glass substrates[11, 12, 13, 14]. We employ sector mirrors consisting of a part of an entire annulus, which enable access of metrology and precision polish equipment to the mirror surface much easier than that with an annular shape. Figure 1 depicts evolution in spatial resolution of grazing-incidence X-ray telescopes for the Sun. We aim to realize sub-arcsecond imagery of the soft X-ray corona of the Sun around the year 2020. In section 2, target specification of the mirror for future solar observations is summarized. In section 3, we describe our latest result on the precision polish in the year 2014 that was made following the first attempt in 2013[14], together with the result from the X-ray measurements on the focusing performance. In section 4, we review the result of the X-ray measurement and discuss possible improvements for mirror fabrication that we are considering, followed by summary in section 5.

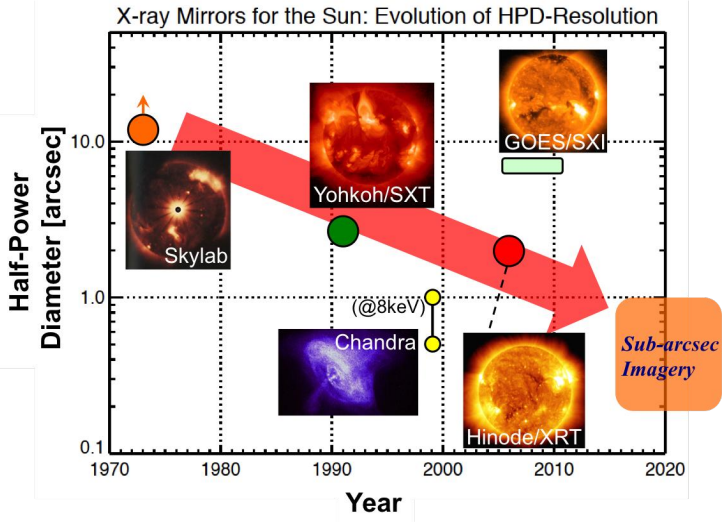

Figure 1. Progress in HPD angular resolution of grazing-incidence soft X-ray mirrors for solar observations. HPD of each telescope mirror is plotted against its year of launch. Data points for *Chandra* X-ray observatory are also shown for comparison.

2. SOFT X-RAY WOLTER MIRRORS FOR FUTURE SOLAR OBSERVATIONS

Scientific objectives to be addressed with sub-arcsecond imagery of the soft X-ray solar corona, in particular those coupled with photon-counting capability for the focal-plane detector, are discussed in Sakao et al. 2014[14] together with target specification for the X-ray Wolter mirror. In addition to sub-arcsecond imaging performance to resolve fine structures of hot plasmas in the corona, combination with photon-counting (imaging-spectroscopy) capability covering up to ~10 keV is particularly powerful in investigating magneto-hydrodynamic structures, such as possible fast/slow shocks, in flares and could even address generation process(es) of supra-thermal electrons out of thermal plasmas in the corona that will eventually emit hard X-rays as they are accelerated. Table 1 summarizes target specification of precision Wolter I mirrors for future observations of the Sun. Towards this goal, a series of engineering mirrors are being developed followed by evaluation of X-ray imaging performance which are described in the next section.

Table 1. Target specification of precision soft X-ray Wolter I mirrors for future observations of the solar corona.

Item	Description	Note
Energy range	~0.5 − ~10 keV	
Angular resolution	< 1" HPD	Defined at 2 and 8 keV
Off-axis scattering	$\lesssim 10^{-5}$ of the PSF peak at 1 arcmin off-axis position	Defined at 8 keV
Geometric area	~1.5 cm^2 (TBD)	

3. ENGINEERING MIRROR IN 2014

Design parameters for the engineering mirror

Following fabrication and subsequent measurement in X-rays of the first engineering Wolter I mirror (Engineering Mirror #1; Sakao et al. 2014[14]), the second engineering Wolter I mirror (Engineering Mirror #2) was fabricated. Particular attention was made for the fabrication of the second mirror in its focusing performance near the higher end of the energy range (8 keV) as the slope error in the surface figure around the spatial scale of ~1 mm resulted in poor focusing performance for the first mirror. The precision polish was made by combination of a deterministic polishing method (MRF; Magnetorheological Finishing[15]) and smoothing while metrology of the surface figure by combining mechanical and optical/interferometric measurements with spatial-scale-dependent filters applied to the metrology results to take into account efficiency and long-term trend of each measurement method.

Figure 2 shows Engineering Mirror #2 after precision polish and coating. Coating with platinum was made in limited portions of the mirror substrate (32.5 mm along the optical axis direction while 10 mm along the cylindrical direction for both parabola and hyperbola sections) where final polish was made with an improved polishing head of MRF. One of the sides of the mirror substrate was finished to serve as reference surfaces that represents the mirror optical axis with respect to the incident X-ray beam. Table 2 summarizes design parameters for Engineering Mirror #2. These parameters are mostly originated from a possible future solar X-ray telescope discussed in previous literatures[11, 12, 13, 14].

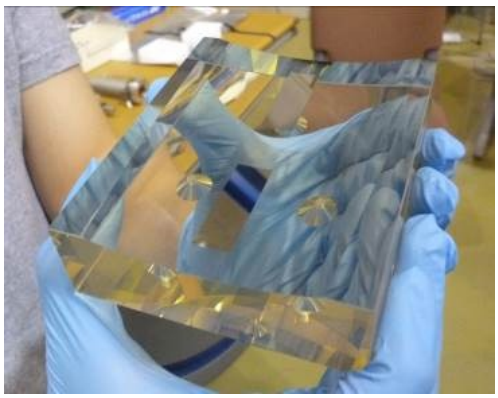

Figure 2. Engineering Mirror #2 of Wolter I optics fabricated in 2014. The farther half of the mirror is the parabola section while the nearer half is the hyperbola section. Coating with platinum was made on a 32.5 mm × 10 mm area for each of the parabola and hyperbola sections.

Table 2. Design parameters for Engineering Mirror #2.

Item	Description	Note
Substrate	CLEARCERAM-Z HS	
Focal length	4000 mm	
Plate scale	1" / 20 μm	
Surface figure profile	Pure Wolter I	
Grazing-incidence angle	0.45 deg.	Angle at the parabola-hyperbola intersection
Mirror reflection area	32.5 mm × 10 mm for both parabola and hyperbola sections	(Along optical axis direction) × (Along cylindrical direction)
Arc radius	125.7 mm	Radius of curvature of the mirror surface along the cylindrical direction
Arc angle	4.6 deg.	Angle sustained by the mirror width (along the cylindrical direction) from the optical axis
Coating	Pt 100 nm + Cr 10 nm for binding layer	Coated by vapor deposition

X-ray measurement on the mirror performance

Following the completion of the Engineering Mirror #2, the mirror was put to X-ray measurement in February 2015 at BL29XUL beamline[16] of SPring-8 synchrotron facility. The measurement was made with 8 keV X-rays (Figure 3). The experiment hatch used for the measurement is separated by 1 km from the synchrotron storage ring, providing highly parallel beam of X-rays. Furthermore, this beamline is designed to provide X-rays of high spatial coherence thus wave-optical calculations can be applied in interpreting and predicting focused beam profiles from surface figure profiles of mirrors.

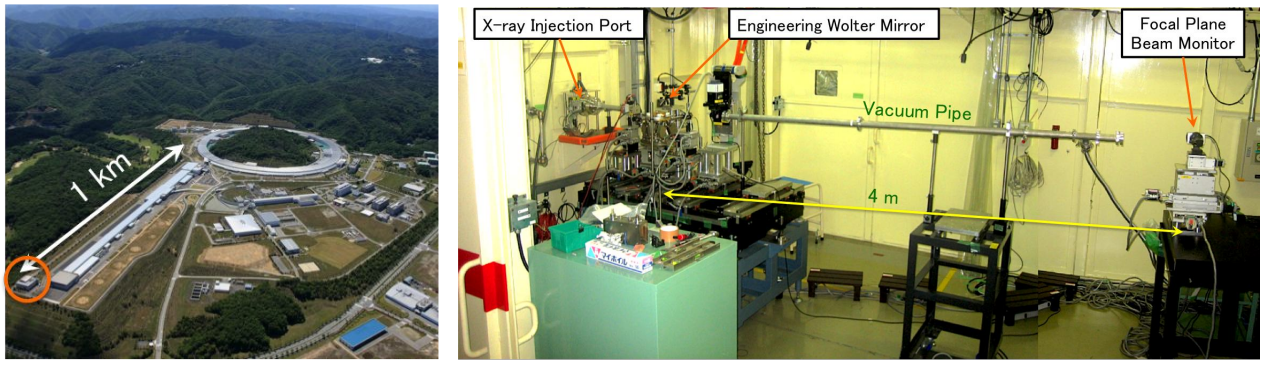

Figure 3. *Left*: Outlook of SPring-8 synchrotron beam facility together with the location of the BL29XUL experiment hatch (EH4; shown by an orange circle) where the X-ray measurement was made. *Right*: Measurement configuration in the experiment hatch.

The Engineering Mirror #2 was placed close to the injection port of synchrotron X-rays in the experiment hatch, mounted on a precision 6-axes stage (hexapod; Figure 4). Area of X-ray illumination onto the mirror was controlled by a slit mechanism with which beam size of X-rays can be adjusted both in horizontal and vertical directions. An ionization chamber was placed in between the slit mechanism and the mirror to monitor the intensity of the incident X-rays to the mirror by measuring the amount of air ionization by the X-ray beam.

A focal-plane beam monitor (called BM2), which consists of a visible-light CMOS image sensor with a scintillator (Ce:YAG ceramics of 100 μm thickness), was placed 4 m away from the mirror, at the focus position. The physical pixel

size of the image sensor was 1.25 μm while it was effectively 2.5 μm because of a 2× magnifier optics located in front of the sensor. A vacuum pipe, tilted by 1.8 degrees (four times the grazing-incidence angle), was inserted in between the mirror and BM2 along the ray path to suppress air attenuation of the reflected X-rays. A polyimide window of 75 μm thickness was attached to each end of the pipe for vacuum seal while maintaining good X-ray transmission. Alignment of the mirror with respect to the incident X-ray beam was made by adjusting the 6-axes stage while monitoring on BM2 the X-ray shadow of the reference surfaces on the mirror substrate.

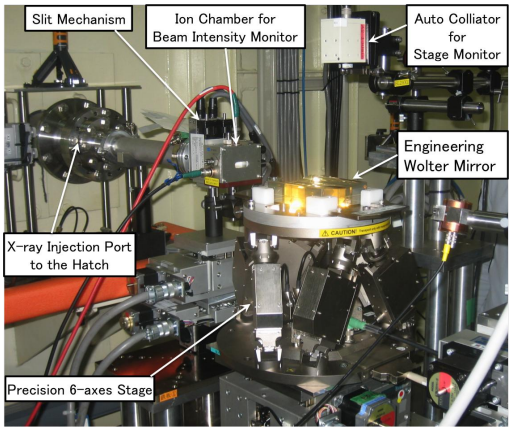

Figure 4. Instrument configuration around Engineering Mirror #2 at Spring-8 BL29XUL. X-rays injected from the left side of the figure (from the "X-ray Injection Port") pass through the slit mechanism and the ionization chamber, reflected by the mirror mounted on a precision 6-axes stage (hexapod), and then proceed to the right towards the focal-plane detector.

Figure 5 shows X-ray intensity distribution in logarithmic scale at the best on-axis focus position for sagittal (in-plane) focusing as measured by BM2. The slit mechanism in front of the mirror was set to have an incident beam size of 240 μm (vertical) × 10 mm (horizontal) to illuminate the entire portion of the parabola section of the mirror.

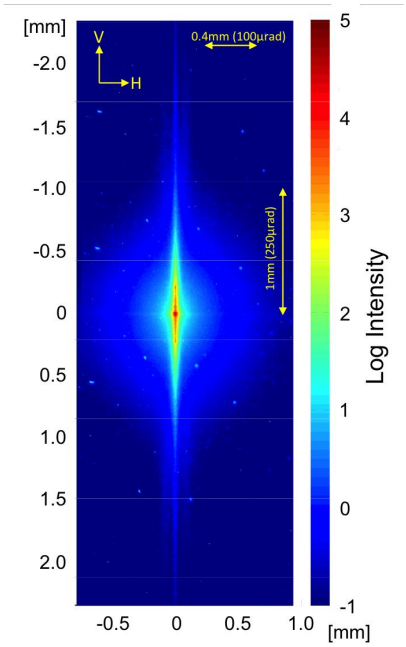

Figure 5. Intensity distribution of 8 keV X-rays in logarithmic scale at the best on-axis focus position for sagittal focusing of the mirror. Bright dots that scatter across the image are likely to be noise originated by the beam monitor BM2.

For the measurement of detailed intensity profiles in and around the PSF core, knife-edge scans were used instead of BM2 as X-ray spots measured with BM2 were diffused by ~3-4 μm due to the thickness of the scintillator in front of the image sensor. When performing knife-edge scans, a PIN photo-diode was set instead of the BM2 detector and intensity profiles were obtained from PIN output current normalized by the ionization chamber current at different positions of the knife edge placed in the focusing X-rays. For both sagittal and meridional (off-plane) focusing, the FWHM size of the focus profile reached as small as 4 μm, corresponding to an angular scale of 0.2" with the focal length of 4 m (Figure 6, left panel).

On the other hand, there was large amount of small-angle scattering (distributing right outside the PSF core) with which HPD of the intensity profile remained at ~3". Furthermore, there was notable difference in focus position along the optics axis between the sagittal and the meridional focusing (*i.e.*, large astigmatism); the meridional focal length was shorter by ~40 cm as compared to the designed length of 4 m.

For large-angle scattering, the measurement was made with BM2. The right panel of Figure 6 indicates a preliminary profile of the scattering wing along the meridional direction at the sagittal best focus. For this wing profile measurement, the slit mechanism in front of the mirror was set to have an incident beam size of 240 μm × 1 mm. The wing profile was made as a composite of intensity profiles with different exposure times (30 ms, 1 s, 10 s, and 1 min.) for BM2. As it was likely that there was excess fluorescent light from the scintillator generated by the intense focusing core, which could have affected low-level wing signals, the result shown here should still be regarded as preliminary. Nonetheless, we may expect that the mirror has attained a scattering level of well below 10^{-4} at 1 arcmin off-axis position.

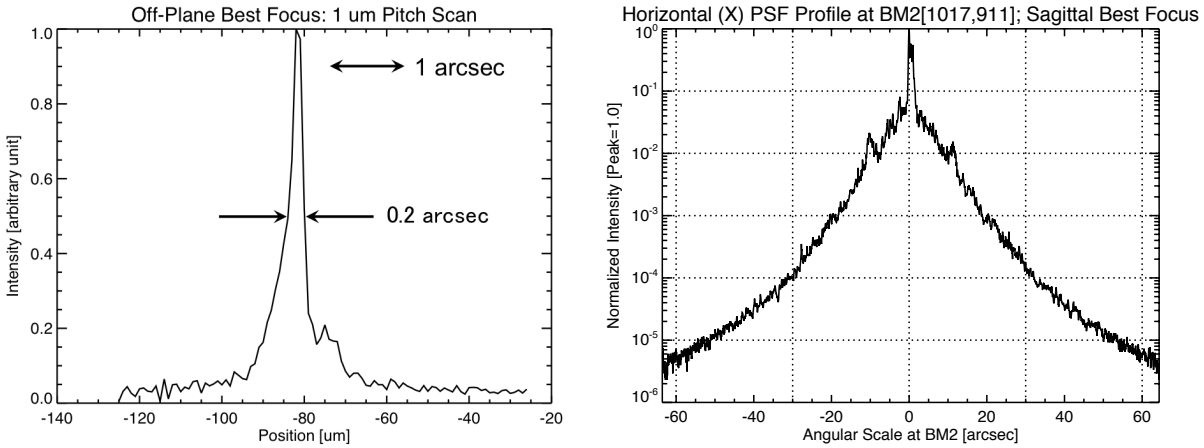

Figure 6. *Left*: X-ray beam profile at the best focus position for meridional focusing, as derived from a knife-edge scan of 1 μm pitch. The FWHM beam size reached as small as 0.2". *Right*: Scattering wing profile of the mirror along the meridional direction at the sagittal best focus measured with BM2. Although preliminary, the wing profile reached a scattering level of well below 10^{-4} at 1 arcmin (60") off-axis position. Small spikes seen at around ±10" off-axis positions are due to periodic residuals of the surface figure error caused by the mirror polishing process.

4. PROSPECTS FOR FUTURE IMPROVEMENT

X-ray measurements at 8 keV at SPring-8 BL29XUL on Engineering Mirror #2 provided the following findings.

1. The FWHM size of the PSF core reached as small as 4 μm, corresponding to an angular scale of 0.2", at each of the sagittal and meridional best on-axis focus positions.
2. The HPD size of the focus profile remained at ~3" (~60 μm) due to a large amount of small-angle scatter just outside the PSF core.

3. There was significant astigmatism present between the sagittal and meridional focusing with which the best meridional focus position was shifted towards the mirror by ~10% (~40 cm) of the designed focal length.

4. Although preliminary, large-angle scattering profiles indicate that the scattering level at 1 arcmin off-axis position is well below 10^{-4} of the PSF peak.

The presence of large small-angle scatter (Item 2 above) is due to ripples in the figure error present in around ~1 mm^{-1} spatial frequency range. Figure 7 shows PSD profile of surface figure error for Engineering Mirror #2, with that for Engineering Mirror #1 shown in gray for comparison. There is notable improvement in the lower spatial frequency range (below 1 mm^{-1}) with which the FWHM size of the PSF core was improved as compared to the first mirror[14]. Also, improvement was achieved in the spatial frequency range above 3 mm^{-1} which led to the improved scattering wing profile. However, not much improvement has yet been made in the spatial frequency range of ~1 mm^{-1} to ~3 mm^{-1} which resulted in the large amount of small-angle scattering. Wave-optical calculations indicate that if we were successful in reducing amplitudes of surface figure errors by a factor of 2 in the 0.3-3 mm^{-1} range, we expect sub-arcsecond HPD size for the focus profiles. This is our next target for the precision polish.

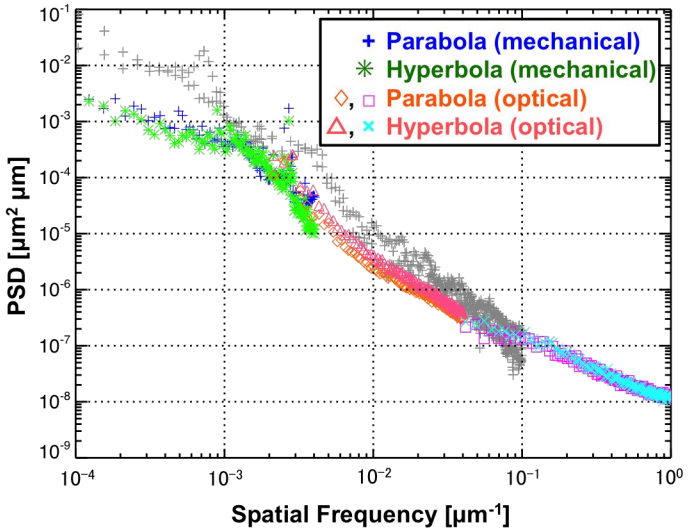

Figure 7. PSD profile of surface figure error for Engineering Mirror #2 (shown in colors), from mechanical and optical/ interferometric measurements employed for lower and higher spatial frequencies, respectively. PSD profile for the first engineering mirror (Engineering Mirror #1) is also shown in gray.

Another major issue with Engineering Mirror #2 is that there was large astigmatism present between sagittal and meridional focusing (Item 3). The deviation in focal length for meridional focusing corresponds to an incorrect radius of curvature in the meridional direction introduced by an error in sag of only 6.5 nm in the mirror area. This small error then might be originated from errors in the absolute position accuracy which may be quite hard to remove. We are considering to correct the astigmatism by performing post-measurement deposition coating in which surface figure is to be corrected by controlling coating thicknesses.

5. SUMMARY

The Engineering Mirror #2 fabricated in 2014 showed good focusing performance in terms of FWHM spot size while its HPD size still fell short of sub-arcsecond spatial resolution. Furthermore, there was a major issue of large astigmatism present between sagittal and meridional focusing. We have devised an improved polishing approach to reduce figure error amplitudes in the spatial frequency range around 1 mm^{-1} and suppress small-angle scatter just outside of the PSF

core. The improvement in precision polish includes (1) improvement in the MRF polishing head with which the deterministic polish is expected to cover spatial frequency range up to ~2 mm^{-1} and (2) improvement in smoothing with which figure error amplitudes for the range above ~2 mm^{-1} are expected to be further reduced.

As for the large astigmatism revealed by the X-ray measurement, this could have been caused by errors in the absolute position accuracy when fabricating the mirror. As this amount of absolute error is extremely hard to remove during fabrication, our approach is to adjust focal length of meridional focusing, after focal-length measurement in X-rays, by adjusting meridional radius of curvature with controlled deposition onto the mirror surface.

The above set of improvement is planned to be carried out in the 2015-2016 time frame with which, once successful, engineering demonstration of sub-arcsecond Wolter mirror in the ~0.5 − ~10 keV energy range for future solar observations will be accomplished. Meanwhile, as a step towards observations from space with a satellite, we are seeking for flight opportunities to verify in-flight performance of our sub-arcsecond Wolter mirror(s) with a sub-orbital mission such as NASA's LCAS (Low Cost Access to Space) program.

ACKNOWLEDGEMENTS

The X-ray mirror development activities have been supported by the Japanese Ministry of Education, Science, Sports and Culture, Grant-in-Aid for Challenging Exploratory Research, 24654053, and Grant-in-Aid for Scientific Research (A), 26247031. We are also grateful to the support so far made from the strategic R&D fund for future space missions from ISAS/JAXA Space Sciences Steering Committee.

REFERENCES

[1] Tsuneta, S., Takahashi, T., Acton, L. W., Bruner, M. E., Harvey, K. L., and Ogawara, Y., "Global Restructuring of the Coronal Magnetic Fields Observed with the Yohkoh Soft X-Ray Telescope," PASJ 44, L211-L214 (1992).
[2] Masuda, S., Kosugi, T., Hara, H., Tsuneta, S., and Ogawara, Y., "A loop-top hard X-ray source in a compact solar flare as evidence for magnetic reconnection," Nature 371, 495-497 (1994).
[3] Tsuneta, S., Masuda, S., Kosugi, T., and Sato, J., "Hot and Superhot Plasmas above an Impulsive Flare Loop," Ap. J. 478, 787-798 (1997).
[4] Gosling, J. T., "The Solar Flare Myth," JGR-A 98, 18937-18949 (1993).
[5] Klimchuk, J. A., "Key aspects of coronal heating," Phil. Trans. R. Soc. A 373, 20140256, 16pp (2015).
[6] Hara, H., Watanabe, T., Harra, L. K., Culhane, J. L., Young, P. R., Mariska, J. T., and Doschek, G. A., "Coronal Plasma Motions Near Footpoints of Active Region Loops Revealed from Spectroscopic Observations with *Hinode* EIS," Ap. J. Lett. 678, L67-L71 (2008).
[7] Cirtain, J. W., Golub, L., Winebarger, A. R., De Pontieu, B., Kobayashi, K., Moore, R. L., Walsh, R. W., Korreck, K. E., Weber, M., McCauley, P., Title, A., Kuzin, S., and DeForest, C. E., "Energy release in the solar corona from spatially resolved mangetic braids," Nature 493, 501-503 (2013).
[8] Wolter, H., "Spiegelsysteme streifenden Einfalls als abbildende Optiken für Röntgenstrahlen," Ann. der Physik 445, 94-114 (1952).
[9] Misaki, K., Hidaka, Y., Ishida, M., Shibata, R., Furuzawa, A., Haba, Y., Itoh, K., Mori, H., and Kunieda, H., "X-ray telescope onboard Astro-E. III. Guidelines to performance improvements and optimization of the ray-tracing simulator," Applied Optics 44, 916-940 (2005).
[10] Zissa, D. E., "AXAF-I High Resolution Mirror Assembly image model and comparison with x-ray ground-test image," Proc. SPIE 3766, 36-50 (1999).
[11] Sakao, T., Narukage, N., Shimojo, M., Tsuneta, S., Suematsu, Y., Miyazaki, S., Imada, S., Nishizuka, N., Watanabe, K., Dotani, T., DeLuca, E. E., and Ishikawa, S., "Photon-counting soft X-ray telescope for the Solar-C mission," Proc. SPIE 8148, 81480C, 13 pp. (2011).
[12] Sakao, T., Narukage, N., Imada, S., Suematsu, Y., Shimojo, M., Tsuneta, S., DeLuca, E. E., Watanabe, K., and Ishikawa, S., "The X-ray/EUV telescope for the Solar-C mission: Science and development activities," Proc. SPIE 8443, 84430A, 11 pp. (2012).
[13] Sakao, T., Narukage, N., Shimojo, M., Watanabe, K., Suematsu, Y., Imada, S., and Ishikawa, S., "The soft X-ray photon-counting spectroscopic imager for the Sun," Proc. SPIE 8862, 88620T, 12 pp. (2013).

[14] Sakao, T., Narukage, N., Suematsu, Y., Watanabe, K., Shimojo, M., Imada, S., Ishikawa, S., and DeLuca, E. E., "The soft x-ray photon-counting telescope for solar observations," Proc. SPIE 9144, 91443D, 8 pp. (2014).
[15] Harris, D. C., "History of Magnetorheological Finishing," Proc. SPIE 8016, 80160N, 22pp. (2011).
[16] Ishikawa, T., Tamasaku, K., Yabashi, M., Goto, S., Tanaka, Y., Yamazaki, H., Takeshita, K., Kimura, H., Ohashi, H., Matsushita, T., and Ohta, T., "One km beamline at SPring-8," Proc. SPIE 4145, 1-10 (2001).